Supplementary Materials for

Blockade of Chronic Type I Interferon Signaling to Control Persistent LCMV Infection

Elizabeth B. Wilson, Douglas H. Yamada, Heidi Elsaesser, Jonathan Herskovitz, Jane Deng, Genhong Cheng, Bruce J. Aronow, Christopher L. Karp, David G. Brooks*

*Corresponding author. E-mail: dbrooks@microbio.ucla.edu

Published 12 April 2013, *Science* **340**, 202 (2013)
DOI: 10.1126/science.1235208

This PDF file includes:

SUPPLEMENTARY MATERIALS

MATERIALS and METHODS

Mice and Virus: C57Bl/6 (wild type) mice were purchased from The Jackson Laboratory (Bar Harbor, ME). *Ifnar1*-/- mice were provided by Dr. Genhong Cheng and Dr. Dorian McGavern (NINDS/NIH). Vert-X IL-10/GFP reporter mice were provided by Dr. Christopher Karp (CCHMC). Six-ten week old mice were used for all experiments. All mice were housed under specific pathogen-free conditions and mouse handling conformed to the requirements of the University of California, Los Angeles Animal Research Committee guidelines. Mice were infected intravenously (i.v) via the retro-orbital sinus with $2x10^6$ plaque forming units (PFU) of LCMV-Arm or LCMV-Cl13. Virus stocks were prepared and viral titers were quantified as described previously(8).

***In vivo* blocking antibody treatments:** C57Bl/6 mice were treated ip with IFNR1 blocking antibody (clone MAR1-5A3; Leinco Technologies, St. Louis MO) either starting prior to infection: day -1 (500μg), day 0 (500μg), day 2 (250μg), day 4 (250μg) and day 6 (250μg) or therapeutically in the midst of the established persistent infection: day 25 (500μg), day 27 (500 μg), and day 29 (250μg). In some experiments C57BL/6 mice were depleted of CD4 T cells prior to infection with anti-CD4 antibody (clone YTS; BioXCell, West Lebanon NH) at day -5 (250μg) and day -1 (250μg). For IFNγ depletion C57Bl/6 mice were treated with 500μg anti-IFNγ antibody (clone XMG1.2; BioXCell, West Lebanon NH) on day -1, 3 and 6 after LCMV-Cl13 infection.

Cytokine Quantification: IL-10, IFNγ and IL-18 levels were determined using cytokine specific Quantikine ELISA kits (R & D Systems, Minneapolis, MN). Optical density values were read using a Synergy 2 plate reader (BioTek, Winooski, VT) at 450nm. Luminex was performed using the MILLIPLEX MAP Mouse Cytokine/Chemokine 22-plex kit (Millipore, Billerica, MA). Samples were analyzed on a Bio-Plex 200 System with HTF and Bio-Plex Manager 6.1 Software (Bio-Rad, Hercules, CA).

RNA microarray: C57Bl/6 mice were either left uninfected (naïve) or infected with LCMV-Arm or LCMV-Cl13 (n=3-4 mice per group). Spleens were isolated on day 5, 9 and 30 after infection and immediately

frozen in RNA Later (Qiagen) at 1mg/ml tissue. Whole spleens were subsequently homogenized, and RNA from splenic homogenates was isolated with the RNeasy extraction kit (Qiagen). RNAs were evaluated using an Agilent Bioanalyzer, labeled using the Ambion WT labeling kit, and hybridized to the Affymetrix Mouse Genes ST 1.0 microarray which were scanned and summarized using Affymetrix Expression Console and RMA16. RMA normalized data was referenced to uninfected spleen samples and genic probesets with RMA>6.0 that differed between the different sample treatments were identified using ANOVA with Benjamini Hochberg FDR -corrected $p<0.05$ and further ranked by relative fold-differences between LCMV-Arm and Cl13 infected sample groups.

Flow cytometry: Analysis of immune cell subsets was performed by staining directly *ex vivo* for surface expression of CD45-Pacific Orange or Pacific Blue, CD11c-Pacific Blue or PE, Thy1.1-FITC or PE, Thy1.2-PerCP, NK1.1-PerCPCy5, B220-APCCy7, CD11bPeCy7, F4/80-PE or APC, MHC Class II-PE, CD4-Pacific Blue, CD8-Pacific Blue all obtained from BioLegend or BD Pharmingen. MHC tetramers were obtained from the NIH. IL-10 expression was determined by GFP expression in the Vert-X IL-10-GFP reporter mouse. Active caspase 1 was quantified by flow cytometry utilizing the FAM-FLICA Caspase-1 activity kit from (Immunochemistry, Bloomington, MN). LCMV viral antigen was quantified by flow cytometric analysis using the anti-LCMV nucleoprotein-specific antibody mAb113. Flow cytometric analysis was performed using a Digital LSR II or FACSVerse (Becton Dickinson).

Purification of dendritic cells and macrophages: IL-10 producing and non-producing DC and macrophages were sorted from spleen following B cell depletion (CD19 MACS beads, Miltenyi) as follows: IL-10 expressing DC (GFP+, CD45+, Thy1.2-, NK1.1-, CD11c+ bright), non-IL-10-producing DC (GFP-, CD45+, Thy1.2-, NK1.1-, CD11c+ bright); IL-10 expressing macrophage (GFP+, CD45+, Thy1.2-, NK1.1-, F4/80+), and non-IL-10 producing macrophages (GFP-, CD45+, Thy1.2-, NK1.1-, F4/80+). Cells were sorted using a FACSVantage fluorescence-activated cell sorter (Becton Dickinson). Post sort purity was >98%.

IFNβ treatment *in vitro*: Bulk splenocytes were cultured in complete media supplemented with recombinant IFNβ (PBL Interferon, Piscataway, NJ) at a concentration of 250 units/mL for 24 hours.

Histology: Naïve and day 9 LCMV-Cl13 infected IFNR1 blocking antibody or isotype treated spleens were excised and fixed for 24hours in 4% paraformaldehyde, then paraffin embedded, sectioned and stained with Hematoxylin and Eosin (H & E). Embedding, H & E staining and tissue scanning for image analysis were performed by the Translational Pathology Core Laboratory at UCLA.

Quantitative RT-PCR: RNA purified from sorted dendritic cells or macrophages, whole splenocytes, or tissue homogenates was isolated with the RNeasy extraction kit (Qiagen). RNA was normalized for input and amplified directly using the One-Step RT-PCR kit (Qiagen). Mx1, OAS, IRF3, IRF7, PDL1, and HPRT were amplified using Applied Biosystems *Assays-on-Demand* TaqMan pre-made expression assays. IFNα and IFNβ primer sequences were previously described- IFNα primers amplify multiple IFNα subtypes (30). RNA expression was normalized to HPRT.

LCMV-specific antibody ELISA: To quantify LCMV-specific IgG, LCMV-Cl13 was used to coat 96-well Maxisorp ELISA plates (Nunc) overnight. Plates were blocked with 3% BSA/PBS/0.05% tween-20. Subsequently, plasma isolated from the indicated mice was incubated on the LCMV coated plates. Plates were washed and incubated with an HRP-labeled goat anti-mouse IgG antibody (Invitrogen), followed by the addition of o-phenylenediamine substrate in 0.05 M phosphate citrate buffer. The reaction was stopped with 2N H_2SO_4 and the optical density (O.D.) values were read using an ELISA plate reader (Synergy 2, BioTek) at 490 nm. The concentration of LCMV-specific IgG was interpolated from a standard curve generated from a serial dilution of purified mouse IgG (Invitrogen; 500 ng/ml -0.49 ng/ml) incubated on plates coated with goat anti-mouse IgG (Invitrogen).

Statistical Analysis: Student's *t*-tests (two-tailed, unpaired) and log-rank Mantel-Cox and Gehan-Breslow tests (for clearance curve; Fig 4C) were performed using the GraphPad Prism 5 software (GraphPad Software Inc.).

SUPPLEMENTARY FIGURE LEGENDS

Figure S1: Cytokine and type I interferon expression in the spleen during acute and persistent infection.

(A) Microarray analysis of cytokine gene expression in whole spleen tissue on the indicated day following persistent LCMV-Cl13 compared to acute LCMV-Arm infection. Increase on the y-axis indicates elevated expression in persistent infection compared to acute infection.

(B) Whole spleen microarray analysis showing *IFNα* and *IFNβ* gene expression in LCMV-Arm (red) or LCMV-Cl13 (green) normalized to naïve spleen levels. An increase on the y-axis indicates elevated expression in the specified infection compared to naïve mice. Each bar indicates the average expression of the indicated cytokine for 3-4 mice per group per time point. Error bars are omitted for clarity.

Figure S2: IFN-I signaling supports the immunosuppressive program.

(A) Plasma IL-10 levels (left) and viral titers (right) at the indicated day following LCMV-Cl13 infection in wt (black) and *Ifnar1*-/- (red) mice.

(B) Flow plots demonstrate LCMV nucleoprotein (LCMV Antigen) staining in splenic dendritic cells (left) and macrophages (right) on day 9 after LCMV-Cl13 infection in isotype and IFNR1 blocking antibody treated mice. Bar graphs quantify the percent +/- S.D. of LCMV antigen positive DC (left) and macrophages (right) in the spleen. In (A) and (B) data are representative of the average ± SD of 4-6 mice per group and 2 or more independent experiments.

(C) *PDL1* mRNA expression (left) in FACSorted DC and macrophages following *in vitro* treatment with media (black) or IFNβ (blue). *PDL1* mRNA was normalized to expression of *HPRT* and each group is a pool of cells from 6-8 mice. The results are representative of 2 independent experiments. IL-10 production (right) quantified in the culture supernatant of splenocytes from LCMV-Cl13 infected wt mice stimulated with media alone (black) or with IFNβ (blue) for 18 hours.

(D) Viral titers at day 9 following LCMV-Arm infection of wt vs. *Ifnar1*-/- mice and isotype vs. IFNR1 blocking antibody treated mice. Each symbol in the scatter plot represents an individual mouse with bars indicating the mean of the group. *p <0.05.

Figure S3: IFNR1 blocking antibody treatment alters the immune environment.

Wild-type mice were treated with isotype or IFNR1 blocking antibody beginning 1 day prior to LCMV-Cl13 infection. (A) *OAS* (top), *Mx1* (middle) and *IRF7* (bottom) mRNA expression relative to *HPRT* in spleen (left), liver (middle) and kidney (right) from naïve (white), isotype (black) or IFNR1 blocking antibody treated (red) mice on day 9 after LCMV-Cl13 infection. Bar graphs depict the average ± SD of 4-5 mice per group and 2 independent experiments. Graphs on the right indicate *OAS* and *Mx1* expression in the indicated FACSorted cell populations from isotype (black) or IFNR1 blocking antibody treated (red) mice. Each cell population is a pool from 6 mice and is representative of 2 independent experiments.

(B) The indicated cytokines were quantified by Luminex in the plasma on day 9 post LCMV-Cl13 infection (top). Inflammasome dependent cytokines were quantified in the plasma by Luminex (IL-1β and IL-1α) or ELISA (IL-18) 9 days after infection (bottom). The bar graph indicates the average +/- SD of DC (left) and macrophages (right) exhibiting enzymatically active caspase 1. Each symbol in the scatter plots indicates an individual mouse and data in the bar graphs is representative of 4-5 mice per group and 2 independent experiments.

(C) Whole spleen images. H and E staining of spleen from naïve mice or on day 9 after LCMV-Cl13 infection of mice treated with isotype or IFNR1 blocking antibody. IFNR1 blocking antibody treated animals exhibited highly organized and demarcated splenic red pulp, marginal zone and white pulp regions, whereas isotype treated mice displayed the characteristic loss of structure during persistent infection.

*, p <0.05.

Figure S4. Cellular makeup and antibody production following IFNR1 blockade.

Wild-type mice were treated with isotype or IFNR1 blocking antibody beginning 1 day prior to LCMV-Cl13 infection. (A) Quantification of total splenocytes and the indicated immune subsets in the spleen on day 9 following LCMV-Cl13 infection.

(B) Graphs represent LCMV-specific IgG and total IgG levels in the plasma (ng/ml) on day 9 (left plots) and day 30 (right plots) after infection.

(C) Representative flow plots of LCMV- Np396 (left) and Gp276 (right) tetramer positive responses in isotype of IFNR1 blocking antibody treated mice 9 days after LCMV-Cl13 infection. Each symbol in the scatter plots represents an individual mouse and bar graphs are comprised of 3-5 mice per group. *, $p < 0.05$.

Table S1: IFN signaling is significantly enhanced in persistent compared to acute LCMV infection. *P*-values are shown for microarray analysis for the interferon receptor inducible genes, STAT genes and interferon responsive genes on the indicated day following persistent LCMV-Cl13 compared to acute LCMV-Arm infection. Red highlighting indicates significantly elevated expression in persistent compared to acute infection.

A.

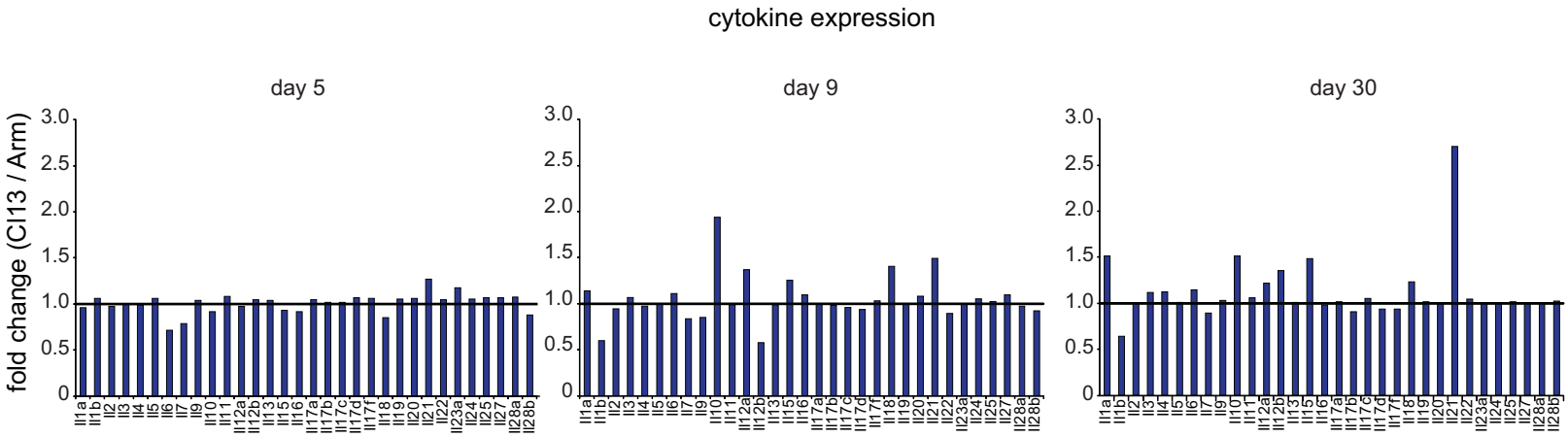
cytokine expression
day 5
day 9
day 30
fold change (Cl13 / Arm)
3.0
2.5
2.0
1.5
1.0
0.5
0
Il1a
Il1b
Il2
Il3
Il4
Il5
Il6
Il7
Il9
Il10
Il11
Il12a
Il12b
Il13
Il15
Il16
Il17a
Il17b
Il17c
Il17d
Il17f
Il18
Il19
Il20
Il21
Il22
Il23a
Il24
Il25
Il27
Il28a
Il28b

B.

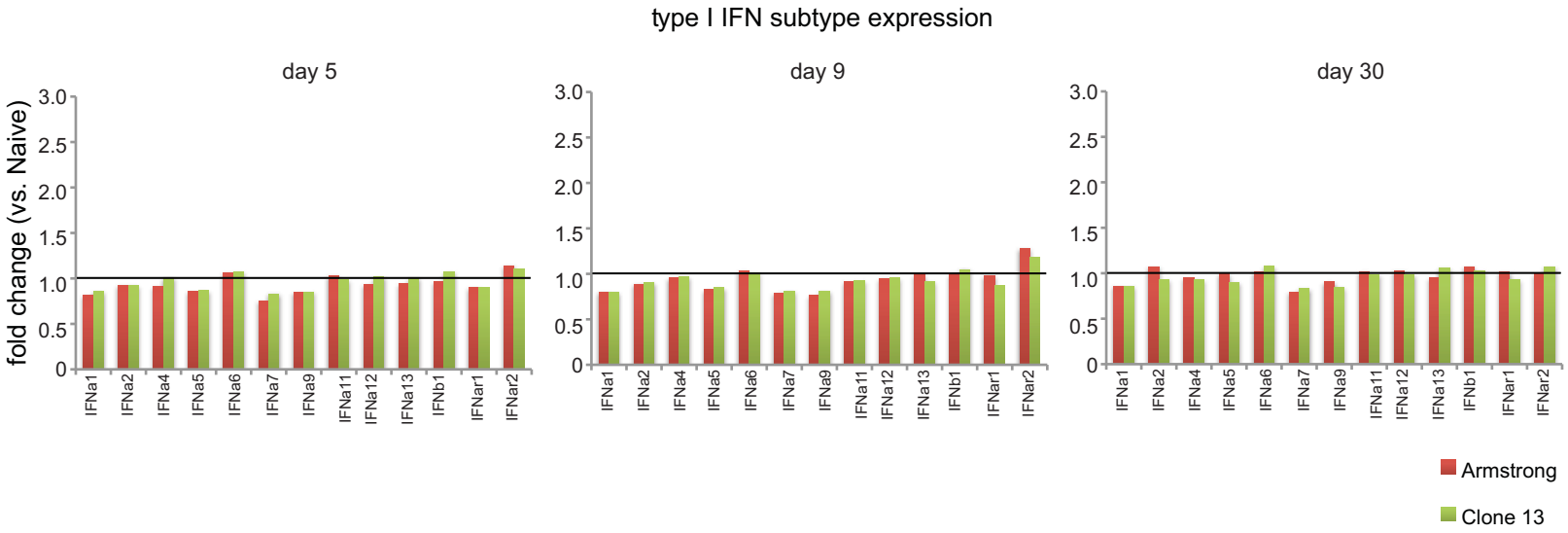
type I IFN subtype expression
day 5
day 9
day 30
fold change (vs. Naive)
3.0
2.5
2.0
1.5
1.0
0.5
0
IFNa1
IFNa2
IFNa4
IFNa5
IFNa6
IFNa7
IFNa9
IFNa11
IFNa12
IFNa13
IFNb1
IFNar1
IFNar2
Armstrong
Clone 13

Figure S1

A.

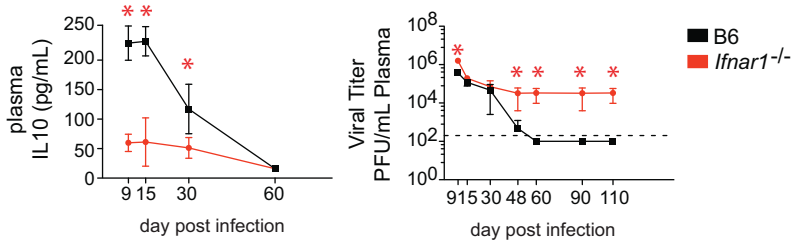

B.

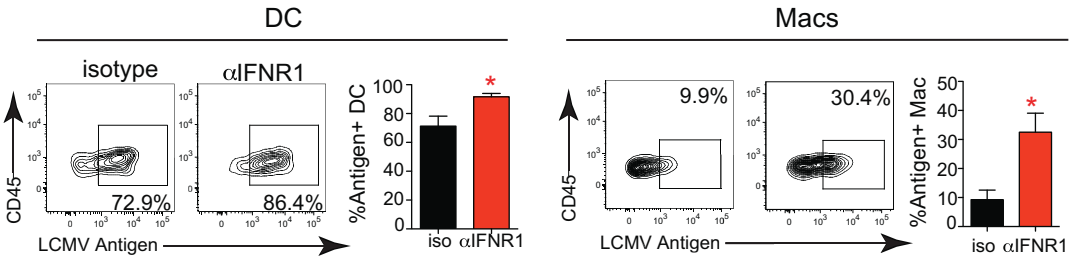

C.

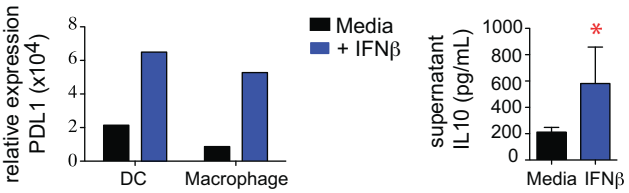

D.

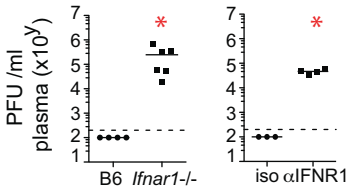

Figure S2

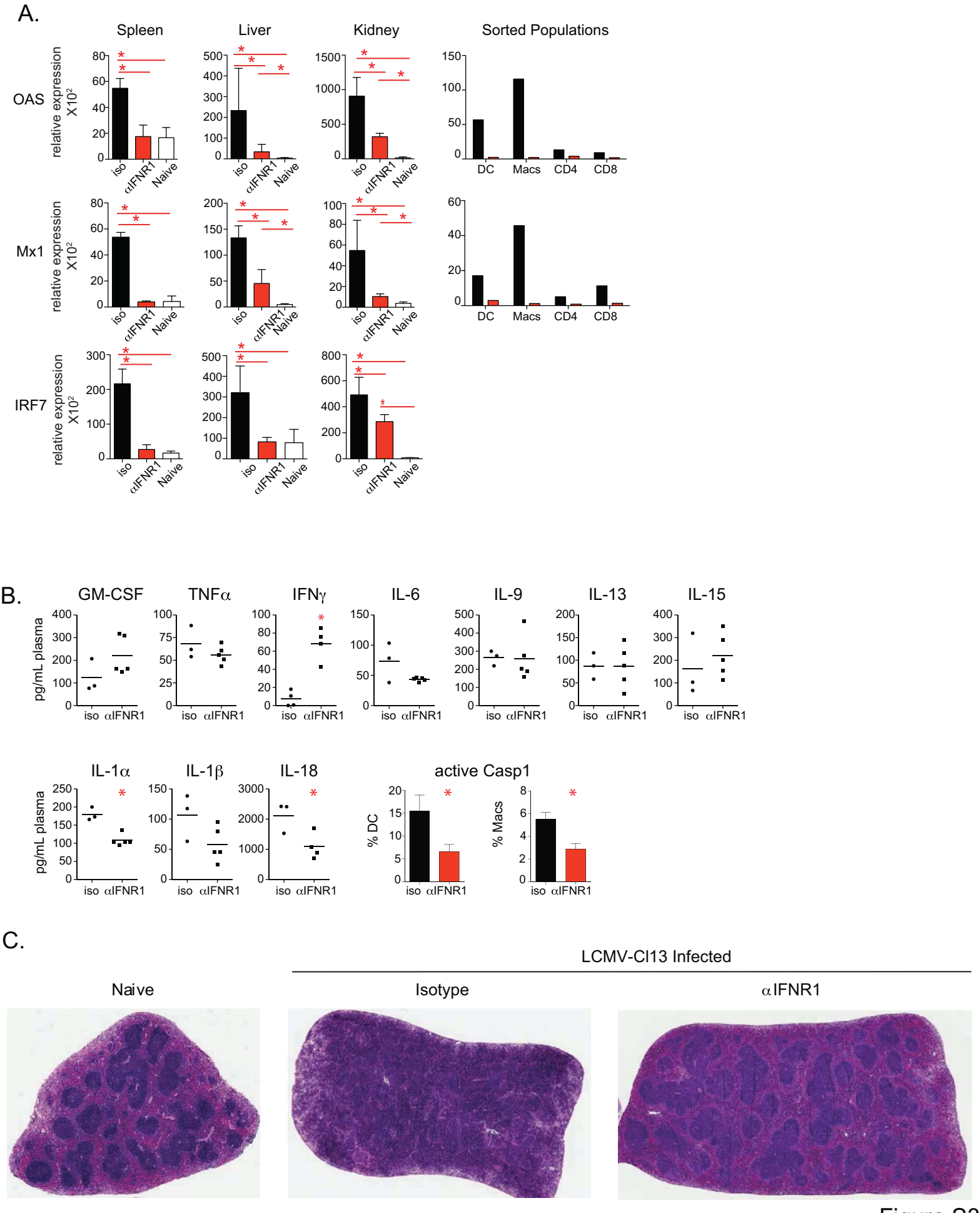
A.
Spleen
Liver
Kidney
Sorted Populations
OAS
Mx1
IRF7
relative expression X10²
iso
αIFNR1
Naive
DC
Macs
CD4
CD8
B.
GM-CSF
TNFα
IFNγ
IL-6
IL-9
IL-13
IL-15
IL-1α
IL-1β
IL-18
active Casp1
pg/mL plasma
% DC
% Macs
C.
LCMV-Cl13 Infected
Naive
Isotype
αIFNR1

Figure S3

A.

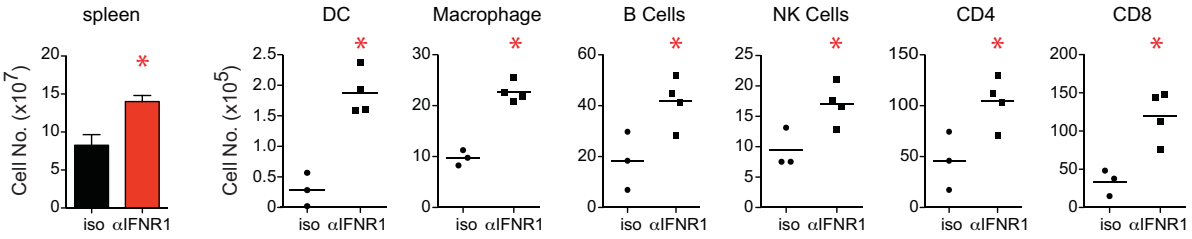

B.

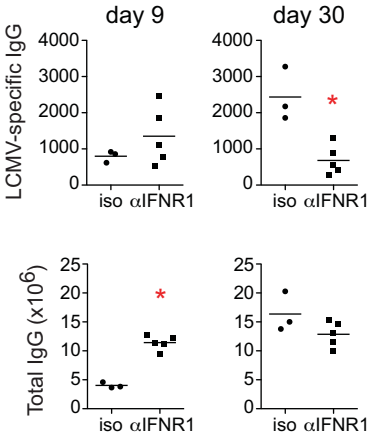

C.

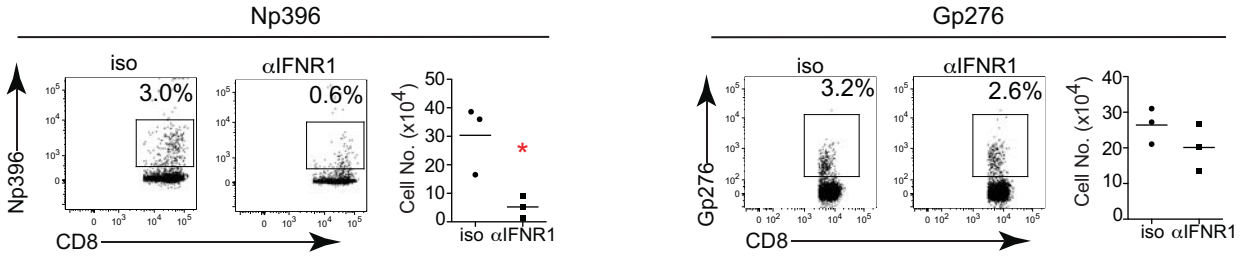

Figure S4

Table S1

IFN-I receptor inducible genes

Gene	day 5	day 9	day 30
Mx2	0.5590	4.0E-05	0.0033
Oas1a	0.3220	0.0035	0.0003
Oas1g	0.7070	0.0004	8.7E-06
Oas2	0.2700	0.0004	2.7E-05
Oas3	0.0250	0.0049	2.8E-05
Oasl1	0.2840	0.0005	0.0001
Oasl2	0.1580	0.0003	2.2E-06

Stat genes

Gene	day 5	day 9	day 30
Stat1	0.0370	0.00323	3.0E-05
Stat2	0.0841	5.8E-05	7.3E-05
Stat3	0.0754	0.0046	0.0020
Stat4	0.1140	0.5520	0.1580
Stat5a	0.0792	0.1460	0.5710
Stat6	0.0492	0.8000	0.8800

IFN-I responsive genes

Gene	day 5	day 9	day 30
IRF1	0.0131	0.0002	0.0059
IRF2	0.1380	0.0083	0.1050
IRF3	0.6590	0.0035	0.6490
IRF4	0.5070	0.0038	3.2E-06
IRF5	0.4500	0.0123	0.7110
IRF6	0.5520	0.1080	0.0320
IRF7	0.7010	0.0022	1.3E-06
IRF8	0.2560	0.0377	0.0005
IRF9	0.5120	0.0005	0.0001

References and Notes

1. E. B. Wilson, D. G. Brooks, Translating insights from persistent LCMV infection into anti-HIV immunity. *Immunol. Res.* **48**, 3 (2010). doi:10.1007/s12026-010-8162-1 Medline

2. Q. Li *et al*., Visualizing antigen-specific and infected cells in situ predicts outcomes in early viral infection. *Science* **323**, 1726 (2009). doi:10.1126/science.1168676 Medline

3. D. L. Barber *et al*., Restoring function in exhausted CD8 T cells during chronic viral infection. *Nature* **439**, 682 (2006). doi:10.1038/nature04444 Medline

4. D. G. Brooks *et al*., Interleukin-10 determines viral clearance or persistence in vivo. *Nat. Med.* **12**, 1301 (2006). doi:10.1038/nm1492 Medline

5. M. Ejrnaes *et al*., Resolution of a chronic viral infection after interleukin-10 receptor blockade. *J. Exp. Med.* **203**, 2461 (2006). doi:10.1084/jem.20061462 Medline

6. C. L. Day *et al*., PD-1 expression on HIV-specific T cells is associated with T-cell exhaustion and disease progression. *Nature* **443**, 350 (2006). doi:10.1038/nature05115 Medline

7. M. A. Brockman *et al*., IL-10 is up-regulated in multiple cell types during viremic HIV infection and reversibly inhibits virus-specific T cells. *Blood* **114**, 346 (2009). doi:10.1182/blood-2008-12-191296 Medline

8. E. B. Wilson *et al*., Emergence of distinct multiarmed immunoregulatory antigen-presenting cells during persistent viral infection. *Cell Host Microbe* **11**, 481 (2012). doi:10.1016/j.chom.2012.03.009 Medline

9. M. Clerici *et al*., Role of interleukin-10 in T helper cell dysfunction in asymptomatic individuals infected with the human immunodeficiency virus. *J. Clin. Invest.* **93**, 768 (1994). doi:10.1172/JCI117031 Medline

10. A. L. Landay *et al*., In vitro restoration of T cell immune function in human immunodeficiency virus-positive persons: effects of interleukin (IL)-12 and anti-IL-10. *J. Infect. Dis.* **173**, 1085 (1996). doi:10.1093/infdis/173.5.1085 Medline

11. E. I. Rigopoulou, W. G. Abbott, P. Haigh, N. V. Naoumov, Blocking of interleukin-10 receptor—a novel approach to stimulate T-helper cell type 1 responses to hepatitis C virus. *Clin. Immunol.* **117**, 57 (2005). doi:10.1016/j.clim.2005.06.003 Medline

12. M. A. Brockman *et al*., IL-10 is up-regulated in multiple cell types during viremic HIV infection and reversibly inhibits virus-specific T cells. *Blood* **114**, 346 (2009). doi:10.1182/blood-2008-12-191296 Medline

13. J. K. Flynn *et al*.; ATAHC Study Group, Early IL-10 predominant responses are associated with progression to chronic hepatitis C virus infection in injecting drug users. *J. Viral Hepat.* **18**, 549 (2011). doi:10.1111/j.1365-2893.2010.01335.x Medline

14. R. Madan *et al*., Nonredundant roles for B cell-derived IL-10 in immune counter-regulation. *J. Immunol.* **183**, 2312 (2009). doi:10.4049/jimmunol.0900185 Medline

15. W. C. Au, P. A. Moore, W. Lowther, Y. T. Juang, P. M. Pitha, Identification of a member of the interferon regulatory factor family that binds to the interferon-stimulated response element and activates expression of interferon-induced genes. *Proc. Natl. Acad. Sci. U.S.A.* **92**, 11657 (1995). doi:10.1073/pnas.92.25.11657 Medline

16. U. Müller *et al*., Functional role of type I and type II interferons in antiviral defense. *Science* **264**, 1918 (1994). doi:10.1126/science.8009221 Medline

17. D. J. Gough, N. L. Messina, C. J. Clarke, R. W. Johnstone, D. E. Levy, Constitutive type I interferon modulates homeostatic balance through tonic signaling. *Immunity* **36**, 166 (2012). doi:10.1016/j.immuni.2012.01.011 Medline

18. G. Guarda *et al*., Type I interferon inhibits interleukin-1 production and inflammasome activation. *Immunity* **34**, 213 (2011). doi:10.1016/j.immuni.2011.02.006 Medline

19. A. Tishon, H. Lewicki, G. Rall, M. Von Herrath, M. B. Oldstone, An essential role for type 1 interferon-gamma in terminating persistent viral infection. *Virology* **212**, 244 (1995). doi:10.1006/viro.1995.1477 Medline

20. M. G. Von Herrath, B. Coon, M. B. Oldstone, Low-affinity cytotoxic T-lymphocytes require IFN-gamma to clear an acute viral infection. *Virology* **229**, 349 (1997). doi:10.1006/viro.1997.8442 Medline

21. A. Tishon, P. Borrow, C. Evans, M. B. Oldstone, Virus-induced immunosuppression. 1. Age at infection relates to a selective or generalized defect. *Virology* **195**, 397 (1993). doi:10.1006/viro.1993.1389 Medline

22. S. Müller *et al*., Role of an intact splenic microarchitecture in early lymphocytic choriomeningitis virus production. *J. Virol.* **76**, 2375 (2002). doi:10.1128/jvi.76.5.2375-2383.2002 Medline

23. S. Moir, T. W. Chun, A. S. Fauci, Pathogenic mechanisms of HIV disease. *Annu. Rev. Pathol.* **6**, 223 (2011). doi:10.1146/annurev-pathol-011110-130254 Medline

24. R. Ou, S. Zhou, L. Huang, D. Moskophidis, Critical role for alpha/beta and gamma interferons in persistence of lymphocytic choriomeningitis virus by clonal exhaustion of cytotoxic T cells. *J. Virol.* **75**, 8407 (2001). doi:10.1128/JVI.75.18.8407-8423.2001 Medline

25. L. Chen *et al*., Hepatic gene expression discriminates responders and nonresponders in treatment of chronic hepatitis C viral infection. *Gastroenterology* **128**, 1437 (2005). doi:10.1053/j.gastro.2005.01.059 Medline

26. M. Sarasin-Filipowicz *et al*., Interferon signaling and treatment outcome in chronic hepatitis C. *Proc. Natl. Acad. Sci. U.S.A.* **105**, 7034 (2008). doi:10.1073/pnas.0707882105 Medline

27. S. E. Bosinger *et al*., Global genomic analysis reveals rapid control of a robust innate response in SIV-infected sooty mangabeys. *J. Clin. Invest.* **119**, 3556 (2009). Medline

28. B. Jacquelin *et al*., Nonpathogenic SIV infection of African green monkeys induces a strong but rapidly controlled type I IFN response. *J. Clin. Invest.* **119**, 3544 (2009). Medline

29. C. R. Bolen *et al*., The blood transcriptional signature of chronic hepatitis C virus is consistent with an ongoing interferon-mediated antiviral response. *J. Interferon Cytokine Res.* **33**, 15 (2013). doi:10.1089/jir.2012.0037 Medline

30. B. Hahm, M. J. Trifilo, E. I. Zuniga, M. B. Oldstone, Viruses evade the immune system through type I interferon-mediated STAT2-dependent, but STAT1-independent, signaling. *Immunity* **22**, 247 (2005). doi:10.1016/j.immuni.2005.01.005 Medline